Induced seismicity in geologic carbon storage

Víctor Vilarrasa[1,2], Jesus Carrera[1,2], Sebastià Olivella[3], Jonny Rutqvist[4] and Lyesse Laloui[5]

[1] Institute of Environmental Assessment and Water Research, Spanish National Research Council (IDAEA-CSIC), Barcelona, Spain

[2] Associated Unit: Hydrogeology Group (UPC-CSIC), Barcelona, Spain

[3] Dept. of Civil and Environmental Engineering, Technical University of Catalonia (UPC-BarcelonaTech), Barcelona, Spain

[4] Energy Geosciences Division, Lawrence Berkeley National Laboratory, CA, USA

[5] Laboratory of Soil Mechanics, École Polytechnique Fédérale de Lausanne (EPFL), Lausanne, Switzerland

Correspondence to: Victor Vilarrasa (victor.vilarrasa@idaea.csic.es)

ABSTRACT

Geologic carbon storage, as well as other geo-energy applications, such as geothermal energy, seasonal natural gas storage and subsurface energy storage, imply fluid injection/extraction that causes changes in the effective stress field and induces (micro)seismicity. If felt, seismicity has a negative effect on public perception and may jeopardize wellbore stability and damage infrastructure. Thus, induced earthquakes should be minimized to successfully deploy geo-energies. However, the processes that trigger induced seismicity are not fully understood, which translates into a limited forecast ability of current predictive models. We aim at understanding the triggering mechanisms of induced seismicity and to develop methodologies to minimize its occurrence through dimensional and numerical analysis. We find that the properties of the injected fluid, e.g., water or CO_2, have a significant effect on pressure buildup evolution and thus, on fracture/fault stability. In addition to pressure changes, the injected fluid usually reaches the injection formation at a lower temperature than that of the rock, inducing rock contraction, thermal stress reduction and stress redistribution around the cooled region. If low-permeable faults cross the injection formation, local stress changes are induced around them which may reduce their stability and eventually cause fault reactivation. To minimize the risk of inducing felt seismicity, we have developed characterization techniques to reduce the uncertainty on rock properties and subsurface heterogeneity both for the screening of injection sites and for the operation of projects. Overall, we contend that felt induced seismicity can be minimized provided that a proper site characterization, monitoring and pressure management are performed.

Keywords: fluid injection, pressure buildup, coupled processes, caprock integrity, fault reactivation

1. INTRODUCTION

The interest in subsurface energy resources, such as geothermal energy, seasonal natural gas storage, subsurface energy storage and geologic carbon storage, has significantly increased as a means to mitigate climate change (IPCC, 2018). In particular, geologic

5   carbon storage has the potential to store large amounts of carbon dioxide (CO_2) in deep geological formations, reducing CO_2 emissions to the atmosphere (Hitchon et al., 1999; Celia, 2017). Such subsurface energy-related activities imply fluid injection/extraction that change the pore pressure and thus, the effective stresses, causing deformation and potentially fracture and/or fault reactivation that may lead to induced (micro)seismicity

10   (Ellsworth, 2013; Grigoli et al., 2017).

Induced microseismicity, i.e., seismicity of such low magnitude that is not felt on the ground surface (typically moment magnitude, $M<2$), is positive if confined within the injection formation because shear slip of fractures enhances permeability (Yeo et al., 1998; Vilarrasa et al., 2011; Rutqvist, 2015). This permeability enhancement permits

15   injecting the same amount of fluid at a lower injection pressure, thus reducing compression costs. However, induced microseismicity should be avoided in the caprock because its sealing capacity could be compromised, which could lead to CO_2 leakage. Additionally, if felt, induced earthquakes may damage wells, buildings and infrastructure and may cause fear and nuisance among the local population (Oldenburg, 2012). As a

20   result of these negative effects, several projects have been cancelled before they entered into operation, such as an enhanced geothermal system at Basel, Switzerland (Häring et al., 2008; Deichmann et al., 2014), a geothermal project at Sankt Gallen, Switzerland (Edwards et al., 2015; Diehl et al., 2017) and the seasonal gas storage project of Castor, Spain (Cesca et al., 2014; Gaite et al., 2016). Thus, felt induced seismic events have to be

minimized, and ideally avoided, in order to achieve a successful deployment of geo-energy projects.

Geologic carbon storage projects, both at large scale and pilot scale, have not induced any felt earthquake to date (White and Foxall, 2016). This lack of felt seismicity may be due

5   to some favorable aspects of CO_2 storage with respect to water injection that will be explained in this paper. Yet, induced microseismicity is common, such as at In Salah, Algeria (Stork et al., 2015; Verdon et al., 2015), Decatur, Illinois (Kaven et al., 2015; Bauer et al., 2016), and Otway, Australia (Myer and Daley, 2011), projects. Despite the previous absence of felt seismicity, proper protocols should be defined and followed to

10   avoid inducing felt earthquakes in future geologic carbon storage projects.

The aim of this paper is to examine the potential causes of induced seismicity in geologic carbon storage and to explain methodologies that can serve to minimize the risk of inducing felt seismic events. First, the potential triggering mechanisms of induced seismicity are explained. Next, the stress state of deep geological formations, the pressure

15   buildup evolution and non-isothermal effects resulting from CO_2 injection are described. Then, how CO_2 injection affects fault stability is analyzed and, finally, subsurface characterization techniques that can be used for minimizing the occurrence of felt induced seismicity are presented.

20   **2. TRIGGERING MECHANISMS**

The basic principle of induced seismicity is that the pressure build-up caused by fluid injection reduces the effective stresses, which brings the stress state closer to failure (Figure 1). If failure conditions are reached, the elastic energy stored in the rock mass is released and a (micro)seismic event is induced. Failure in geomaterials can occur either

in tensile or shear mode (Jaeger et al., 2009). While tensile failure induces microseismic events of such low magnitude that cannot be felt on the ground surface, shear failure may lead to felt earthquakes if a sufficiently large area of a pre-existing fracture or fault is reactivated. Nevertheless, in the cases in which tensile failure is sought, i.e., to create

5   hydraulic fractures in low-permeable rock to enhance its permeability, shear failure of pre-existing faults may also occur, which may induce felt earthquakes associated to hydraulic fracturing operations (Rubinstein and Mahani, 2015). For example, a felt earthquake occurred at the Preese Hall 1 exploration well for shale gas near Blackpool, UK, during hydraulic fracturing because a pre-existing nearby fault was reactivated

10   (Clarke et al., 2014).

In principle, fluid pressure buildup may seem the only mechanism that induces seismicity. Thus, intuition suggests that stability should improve in the vicinity of the injection well after injection is stopped because fluid pressure drops rapidly. Far away from the injection well, fluid pressure continues to rise and thus, pressure-diffusion could explain continued

15   post-injection induced seismicity (Hsieh and Bredehoeft, 1981), observed for example after the stimulation of enhanced geothermal systems (EGS) (Parotidis et al., 2004). However, pressure-diffusion cannot explain why the magnitude of post-injection seismicity is often higher than that induced during injection, e.g., at Basel, Switzerland (Deichmann and Giardini, 2009), at Soultz-sous-Forêts, France (Evans et al., 2005), and

20   at Castor, Spain (Gaite et al., 2016). Even though this high magnitude post-injection seismicity has not been observed in geologic carbon storage projects, its causes should be understood in order to avoid its occurrence. The counterintuitive occurrence of post-injection induced seismicity is due to the fact that fluid injection in the subsurface involves coupled processes that are more complex than just the hydraulic effect:

- The stress state changes in response to pore pressure variations (Streit and Hillis, 2004; Rutqvist, 2012). Specifically, the total stress increases in the direction of flow due to the lateral confinement that opposes to the expansion of the rock in this direction (Zareidarmiyan et al., 2018). This poro-mechanical effect modifies

  5   the initial stress state and thus, the analysis of fault stability cannot be performed as a simple subtraction of the pressure build-up from the initial effective stress state.

- The injected CO_2 usually reaches the injection depth at a colder temperature than that of the rock because CO_2 does not reach thermal equilibrium with the

  10   geothermal gradient along its way down the well (Paterson et al., 2008). As a result, the injection formation cools down around the injection well, inducing a thermal stress reduction that brings the stress state closer to failure conditions (Vilarrasa and Rutqvist, 2017). The magnitude of induced thermal stresses is proportional to the rock stiffness. Thus, induced thermal stresses depend on the

  15   rock type in which fluid is injected, becoming larger in reservoir rocks than in clay-rich caprocks because they are usually stiffer (Vilarrasa and Makhnenko, 2017).

- The stress changes that arise in the storage formation and the caprock as a result of pressure build-up and cooling vary depending on the rock properties and the

  20   contrast between geological layers (Verdon et al., 2011).

- Each (micro)seismic event provokes a stress redistribution around the portion of the fracture or fault that undergoes shear slip (Okada, 1992). This stress transfer controls the distribution of aftershocks in natural seismicity (King et al., 1994) and may be the reason for observed rotations in the direction of the sheared faults

in sequences of induced seismicity during stimulation of EGS (De Simone et al., 2017).

- Not all the shear slip occurring in fractures or faults induces seismic events. Actually, shear slip may occur aseismically (Cornet et al., 1997). This aseismic slip may induce (micro)seismic events away from the slipped surface (Guglielmi et al., 2015).

- Geochemical reactions may alter the frictional strength of faults, which could lead to failure conditions if a fault is weakened. However, laboratory studies have shown that this effect is in general minor (Rohmer et al., 2016), even on fault gouges that have been exposed to acidic conditions for a long period in natural CO_2 reservoirs (Bakker et al., 2016).

- Heterogeneity in the rock type, strength of faults and the stress field, which may present local variations around faults (Faulkner et al., 2006), affect fault stability. However, the knowledge on the role of heterogeneity in induced seismicity is still limited.

All these potential triggering mechanisms are usually neglected because pressure-diffusion is considered sufficient to explain induced seismicity. Though pore pressure diffusion alone may explain certain sequences of induced events (Shapiro et al., 2002), sequences are usually more complex and imply a combination of several coupled processes. For example, cooling-induced stresses resulting from CO_2 entering the storage formation 45 ºC colder than the rock may explain part of the microseismicity detected at In Salah, Algeria (Vilarrasa et al., 2015). Another example is Weyburn, Canada, where the scarce microseismic events (around 200) that were induced in the caprock at the beginning of injection were interpreted to be caused by stress changes resulting from the contrast in stiffness between the reservoir and caprock (Verdon et al., 2011). Thus, when

assessing the potential for induced (micro)seismicity of CO_2 storage projects, all these coupled processes should be considered (Figure 2).

3. STRESS STATE

5   A careful examination of the subsurface stress state reveals that while crystalline rocks are critically stressed, sedimentary rocks are generally not critically stressed (Vilarrasa and Carrera, 2015). Since CO_2 will be stored in sedimentary basins, their absence of criticality of stress implies that a certain pressure buildup and cooling can be applied without reaching failure conditions (Figure 3). However, the stress state at each site

10   should be measured in order to determine the maximum sustainable injection pressure and maximum temperature drop that would lead to a safe CO_2 storage (Rutqvist et al., 2007; Kim and Hosseini, 2014). Thus, stress measurements should be routinely performed during wellbore perforation, determining both the magnitude and orientation of the principal stresses (Cornet and Jianmin, 1995). Once the stress state is known, the

15   range of fault strike and dip that is favorably oriented for reactivation can be determined (Morris et al., 1996). This exercise is crucial to identify faults that may induce large seismic events and to foresee an optimal design of the injection strategy and define mitigation measures (e.g., Birkholzer et al., 2012; Buscheck et al., 2012; Dempsey et al., 2014) if induce seismicity is predicted to possibly occur above a predefined threshold.

20   The dependence of the stress state on the rock type is due to the contrast in the rock stiffness. Since crystalline rocks are much stiffer than sedimentary rock, stresses induced by tectonics mainly accumulate in the crystalline basement. In contrast, the relatively soft sedimentary rocks deform without accumulating large stresses and as a result they do not usually become critically stressed. It goes without saying there may be cases of critically

stressed sedimentary rocks, which may lead to unexpected high seismicity if no stress measurements are performed.

4. PRESSURE BUILDUP EVOLUTION

5   The pressure buildup evolution of CO_2 injection is favorable to achieve a long-term geomechanically stable situation. In contrast to water injection, which yields a linear increase of pressure with the logarithm of time when a continuous flow rate is injected (Theis, 1935), CO_2 leads to a peak at the beginning of injection followed by a relatively constant pressure buildup (Figure 4). Thus, pressure buildup is relatively easy to control

10   in CO_2 injection operations, which should help to minimize induced (micro)seismicity (Vilarrasa and Carrera, 2015). Such pressure evolution has been observed in the field, at Ketzin, Germany (Henninges et al., 2011), numerically (Vilarrasa et al., 2010; Okwen et al., 2011) and analytically (Vilarrasa et al., 2013a).

   The initial sharp increase in pressure buildup is due to a local reduction in permeability

15   caused by the desaturation around the injection well (Figure 4b), which decreases the relative permeability of both CO_2 and water. However, once CO_2 fills the pores around the injection well (Figure 4c), the CO_2 relative permeability rises. Additionally, since CO_2 viscosity is one order of magnitude lower than that of brine, CO_2 can flow easily inside the storage formation, which leads to a constant or even a slight drop in pressure buildup

20   (Figure 4a). This fluid pressure evolution induces the largest effective stress changes in the caprock at the beginning of injection, coinciding with the peak in pressure buildup. Thus, progressively increasing the flow rate at the beginning of injection may avoid the initial peak in pressure buildup, minimizing the effect on the caprock integrity.

Maintaining the caprock integrity in the long-term is also favored by two effects that tend to decrease pressure buildup inside the storage formation: (1) CO_2 dissolution into the resident brine, and (2) brine flow across the low-permeability formations that confine the storage formation, i.e., caprock and base rock (Vilarrasa and Carrera, 2015). On the one

5   hand, when CO_2 dissolves into brine, fluid pressure decreases because the total fluid volume is reduced (Mathias et al., 2011a). As observed in natural analogues, the percentage of CO_2 that may become trapped by dissolution can be as high as 90% in carbonate storage formations (Gilfillan et al., 2009). In the short-term, CO_2 dissolution can also be high in storage formations with high vertical permeability ($k > 10^{-13}$ m^2)

10   because of the formation of gravity fingers of CO_2-rich brine (Riaz et al., 2006; Hidalgo and Carrera, 2009; Pau et al., 2010). On the other hand, caprock permeability at the field scale is two to three orders of magnitude larger than that at the core scale as a result of the presence of fractures and faults (Neuzil, 1994). Thus, resident brine of the storage formation can flow across the caprock and base rock, lowering the pressure buildup inside

15   the storage formation. Though brine can flow through the caprock, CO_2 cannot because of the high entry pressure of clay-rich formations (Benson and Cole, 2008).

5. NON-ISOTHERMAL EFFECTS

In addition to pressure buildup, thermal effects are also relevant in geologic carbon

20   storage because temperature changes induce thermal stresses that affect fracture stability (Vilarrasa and Rutqvist, 2017). CO_2 reaches the bottom of the injection well at a temperature lower than that of the storage formation because CO_2 flow within the well is isenthalpic (Pruess, 2006) and thus, it heats up at a lower rate than the geothermal gradient (Lu and Connell, 2008). As a result, the rock around injection wells cools down (Figure

5b). The advance of the cooling front with respect to the CO_2 plume is retarded because the rock has to be cooled down (compare Figures 5a and 5b) (Bao et al., 2014; LaForce et al., 2015). Cooling mainly advances by advection in the reservoir, but it also extends into the lower portion of the caprock by conduction (Figure 5b). The extent of the cooling

5   region can become of a few hundreds of meters after some decades of CO_2 injection at industrial scale rates, i.e., megaton injection (Vilarrasa et al., 2014). Thus, unless faults are present in the vicinity of the injection well, they will not be directly affected by cooling. Nevertheless, faults placed far from the cooling region may undergo stability changes as a result of the contraction of the cooled rock, which causes a change in the

10   far-field stresses (Jeanne et al., 2014).

The cooling-induced rock contraction and thermal stress reduction approach the stress state towards shear failure conditions and tensile fractures could be formed if the tensile strength was reached (Luo and Bryant, 2010; Goodarzi et al., 2010; 2012; Gor et al., 2013). The temperature-induced stresses are not isotropic, and thus, the effect on fracture

15   stability depends on the stress regime, i.e., normal faulting, strike-slip or reverse faulting (Vilarrasa, 2016). In general, fracture stability becomes more compromised in the reservoir than in the caprock, which may lead to injectivity enhancement while maintaining the caprock sealing capacity (Goodarzi et al., 2015; Vilarrasa et al., 2017a). This favorable situation specially occurs in normal faulting stress regimes (Vilarrasa et

20   al., 2013b; Kim and Hosseini, 2015).

Figure 6 displays the stress changes that are induced in the reservoir and caprock as a result of cooling and how they affect fracture stability in a normal faulting stress regime. Both the vertical and horizontal stresses decrease inside the reservoir within the cooled region. This stress reduction is proportional to the rock stiffness, the rock thermal

25   expansion coefficient and the temperature change. The vertical stress reduction within the

reservoir causes a disequilibrium in this direction because the overburden on top of the reservoir remains constant (Figure 6a). Thus, to satisfy stress equilibrium and displacement compatibility, the horizontal stresses increase in the lower portion of the caprock, tightening it (Figure 6b). As a result of these stress changes, shear failure

5   conditions are reached within the reservoir, but the caprock remains stable (see the Mohr circles in Figure 6). This contrast in stability between the reservoir and the caprock is highlighted in Figure 5c, which shows that plastic strain, i.e., strain that occurs because failure conditions have been reached, only takes place in the reservoir and not in the caprock (for details on the failure surface, see Vilarrasa and Laloui, 2015). Thus, cold

10   CO_2 injection, i.e., in liquid state (Vilarrasa et al., 2013b), should not be feared because the caprock sealing capacity is not compromised.

6. FAULT STABILITY

Faults are present at the field and basin scale, as observed in CO_2 storage projects (e.g.,

15   Vidal-Gilbert et al., 2010; Rutqvist, 2012; Castelletto et al., 2013a). To name a few, (i) a fault or fractured rock zone opened as a result of pressure buildup at In Salah, Algeria, leading to a double-lobe pattern of uplift on the ground (Vasco et al., 2010; Rinaldi and Rutqvist, 2013); (ii) the storage formation at Snøhvit, Norway, was surrounded by low-permeable faults, which limited its storage capacity (Hansen et al., 2013; Chiaramonte et

20   al., 2015); (iii) the Spanish pilot test site at Hontomín contained several minor faults within a few hundreds of meters from the injection well (Alcalde et al., 2013; 2014); and (iv) the pilot test site at Heletz, Israel, is placed in an anticline crossed by two faults, confining the storage formation to a few hundreds of meters (Figueiredo et al., 2015). The nature of these faults, i.e., flow barriers or conduits (Caine et al., 1996), controls the stress

changes occurring around the fault and thus, fault stability (Vilarrasa et al., 2016). Low-permeable faults may lead to the premature closure of storage sites because of pressure limitations on the storage capacity of the formation (Szulczewski et al., 2012). Actually, if multiple low-permeable faults are present and intersecting each other, they will lead to

5   a compartmentalized reservoir (Castelletto et al., 2013b). In such cases, pressure would increase linearly with time (Zhou et al., 2008; Mathias et al., 2011b), eventually leading to fault reactivation, and thus induced seismicity, if injection is maintained at a constant rate (Cappa and Rutqvist, 2011a; Pereira et al., 2014; Rutqvist et al., 2016).

Fault reactivation may enhance fault permeability due to dilatancy by one to two orders

10   of magnitude (Cappa and Rutqvist, 2011b; Guglielmi et al., 2015). This permeability increase raises the question of whether fault reactivation may lead to CO_2 leakage or not. Such assessment should be made site specifically taking into account the hydro-mechanical properties of the rock and faults. Nonetheless, in general, faults crossing sequences of reservoirs and caprocks maintain a low-permeability, at least, in the sections

15   that cross caprocks as a result of the high clay content of the fault (Takahashi, 2003; Egholm et al., 2008). But more importantly, the entry pressure of the fault remains high in the caprock sections (Vilarrasa and Makhnenko, 2017), hindering upwards CO_2 leakage, as observed in numerical simulations that incorporate fault heterogeneity (Rinaldi et al., 2014). Additionally, the stress state of the upper crust, which is

20   characterized by a critically stressed crystalline basement overlaid by non-critically stressed sedimentary rock (recall Section 3), favors nucleation of the largest seismic events in the crystalline basement rather than in the sedimentary rock where CO_2 is stored. This hypocenter distribution has been observed in central US as a result of wastewater injection in the basal aquifer, which implies that permeability enhancement occurs below

the storage formation and thus, fault permeability in the caprock and above it remains

unaltered, limiting the risk of CO_2 leakage (Verdon, 2014).

Apart from CO_2 leakage, the magnitude of the potential induced earthquakes is a concern

because of the damage and fear that they could generate. The magnitude of earthquakes,

5   M, is proportional to the rock shear modulus, the rupture area and the mean shear slip

(Stekettee, 1958). Thus, the magnitude is controlled by the pressurized area of the fault.

In this way, the orientation of the injection well affects the magnitude of potential induced

seismicity because horizontal wells pressurize a larger area than vertical wells, but take a

longer time to exceed the critical pressure at the fault (Rinaldi et al., 2015). The magnitude

10   of induced seismic events is also controlled by the brittleness of the fault. While brittle

faults with a slip-weakening behavior can induce large earthquakes ($M>4$) (Rutqvist et

al., 2016), ductile faults give rise to progressive ruptures in which shear slip progressively

accumulates, giving rise to aseismic slip or a swarm-like seismic activity (Vilarrasa et al.,

2017b).

15   Another aspect that controls fault stability as a result of fluid injection is fault offset.

Figure 7 represents a typical scenario that can be encountered in a normal faulting stress

regime setting, i.e., a steep fault in which the hanging wall has slid downwards with

respect to the footwall. The fault is considered to have an offset equal to half of the storage

formation thickness. The fault is composed by a low-permeable core (10^{-19} m^2) and a

20   damage zone on each side of the core. The properties of the damage zone depend on the

material it is in contact with, becoming more permeable and less stiff than the intact rock

as a result of fracturing. Thus, the damage zone is of high permeability next to the storage

formation, but of relatively low-permeability and high entry pressure next to the caprock

and base rock (Vilarrasa et al., 2016). The caprock and base rock are more deformable

25   than the storage formation. CO_2 is injected at a constant mass flow rate in the hanging

wall, 1 km away from the fault, which leads to the pressurization of the storage formation. After 1 year of injection, the pressure buildup in the hanging wall of the storage formation is of 10 MPa. The low-permeable fault acts as a flow barrier, causing a rapid reservoir pressurization. This pressure increase expands the storage formation. In particular, the

5   pressurized storage formation pushes the fault towards the right-hand side. This expansion is uniform along the whole thickness of the storage formation, but the deformation of the rock on the other side of the fault depends on the stiffness of the surrounding rock. Since the storage formation is stiffer than the base rock, it contracts less than the base rock, but induces larger stresses. As a result, the induced horizontal

10   stresses in the in-plane direction are high where the storage formation is present on both sides of the fault, but it is low where the base rock is on the other side of the fault.

These stress changes have a direct implication of fault stability. Figure 8 displays the changes in the mobilized friction angle around the fault as a result of CO_2 injection. The most destabilized region is the lower half of the pressurized storage formation. Thus, an

15   induced seismic event would be initiated in that region of the fault, but slip may become arrested below the caprock because fault stability improves within the damage zone of the storage formation on the side that is not pressurized. This difference in fault stability can be easily appreciated by representing Mohr circles in these zones (see inset in Figure 8). While the deviatoric stress is maintained in the lower portion of the pressurized storage

20   formation because the horizontal stress in the in-plane direction does not increase (see red circle in Figure 8), the size of the Mohr circle decreases in the upper portion of the pressurized storage formation because of the increase in the horizontal stress in the in-plane direction where the storage formation is placed on both sides of the fault (see green circle in Figure 8). This fault stability analysis highlights the fact that the accurate

assessment of fault stability changes in geologic carbon storage sites completely depend on proper site characterization.

7. CHARACTERIZATION TECHNIQUES

5   Site characterization has traditionally been considered as an activity that should be performed before a projects enters into operation. Though necessary, such previous characterization tests are limited in time and thus, they can only characterize a small volume of rock around the injection well (Niemi et al., 2017). However, the size of the region affected by injection grows with the square root of time and since geologic carbon

10   storage projects are planned to last several decades, full characterization can only be achieved by considering operation as a continuous characterization. This continuous characterization approach is necessary to reduce surface uncertainty in predictive models of felt seismicity.

To assess whether CO_2 injection may induce felt seismicity, it is necessary to characterize

15   the geological media in order to build a conceptual model of the site. This conceptual model should include the geological layers (at least the caprock, potential secondary caprocks, the storage formation and subjacent layers down to the crystalline basement) and faults. Apart from the geometry, the hydraulic (permeability and porosity), thermal (thermal conductivity and heat capacity) and geomechanical (stiffness and strength)

20   properties are required. Additionally, the initial conditions should be determined, i.e., the fluid pressure profile (if pressure is hydrostatic or if there are pressure anomalies), the geothermal gradient, Gutenberg-Richter law and the stress state. Determining the magnitude and orientation (and their variability) of the stress tensor is critical, because fault stability depends on the orientation of a given fault with respect to the stress tensor

(Morris et al., 1996). These properties can be measured in the laboratory from core samples or in the field. While laboratory measurements allow a tight control of test conditions, they usually test only the rock matrix and fail to acknowledge scale effects associated to spatial variability of the above properties and the impact of discontinuities

5   (e.g., Ledesma et al., 1996; Zhang et al., 2006; Cai et al., 2007). Thus, interpretation of field measurements is more representative.

To obtain estimates representative at the field scale of the hydraulic and geomechanical properties, Vilarrasa et al. (2013c) proposed a hydro-mechanical characterization test for CO_2 storage sites (Figure 9). The test consists in injecting water at a high flow rate until

10   microseismic events are induced. Ideally, the same brine from the storage formation should be injected to avoid geochemical reactions around the injection well that may alter rock properties. However, injecting brine would imply having a large surface facility to store the brine from the storage formation that would have been pumped previously. The test has to be closely monitored with pressure, temperature, deformation and

15   microseismicity monitoring. The hydraulic properties of the storage formation and caprock can be determined from the interpretation of injection as a hydraulic test (Cooper and Jacob, 1946; Hantush, 1956). If heterogeneities are present in the storage formation, their effect is only detectable for a limited period of time (Wheatcraft and Winterberg, 1985; Butler and Liu, 1993). For this reason, it is extremely important to continuously

20   measure pore pressure changes during injection. As for the geomechanical properties of the storage formation and caprock, they can be derived from the interpretation of the vertical displacement at the top of the storage formation and the caprock. Additionally, measuring the pressure evolution in the caprock, which undergoes a pressure drop in response of the pressure buildup in the storage formation (Hsieh, 1996), also gives

25   information on the geomechanical properties. The magnitude of this reverse-water level

fluctuation is inversely proportional to the storage formation stiffness (Vilarrasa et al., 2013c). Injection should be maintained until microseismic events are induced in the caprock, which gives an initial estimate of the maximum sustainable injection pressure that should not be exceeded during CO_2 injection to avoid compromising the caprock

5   sealing capacity. This test is valuable to characterize storage sites in a pre-operation stage, but it should be complemented by a continuous site characterization during operation to characterize geological features present in the far field and reduce subsurface uncertainty.

A continuous characterization technique that permits detecting and locating low-permeable faults is that proposed by Vilarrasa et al. (2017c). The idea is to use diagnostic

10   plots, i.e., plots that include the fluid pressure evolution together with the derivative of the fluid pressure with respect to the logarithm of time (Bourdet et al., 1983; Renard et al., 2009), to detect faults significantly before (in the order of days) than if only fluid pressure evolution interpretation would be used (Figure 10a). This early identification of faults should permit decision makers to perform pressure management if necessary to

15   mitigate future induced seismicity. This methodology only detects faults that are at least three orders of magnitude less permeable than the storage formation. However, this should not be a problem in terms of induced seismicity because faults that do not act as a flow barrier induce relatively small changes in fault stability (Vilarrasa et al., 2016). Low-permeable faults generate an additional pressure buildup that differs from the expected

20   pressure evolution in an aquifer that would not contain that fault. Thus, by comparing the measured pressure evolution, and its derivative with respect to the logarithm of time, with the predicted one, low-permeable faults can be detected. This additional pressurization also affects the CO_2 dynamics because CO_2 is pushed away from the direction of the fault, leading to an asymmetric CO_2 plume (Figure 10b). Such asymmetry could be detected at

25   monitoring wells, suggesting the presence of a fault, but it could also be due to reservoir

heterogeneity (Chen et al., 2014). Once a fault is detected and located, it should be incorporated into the conceptual model of the site. Additional characterization techniques may be necessary to obtain a precise information on the detected faults. Then, field measurements should be compared with the updated conceptual model, which will permit

5   identifying and locating new faults (Figure 10c) from the determination of the divergence time and the use of type curves (Figure 10d). Such continuous characterization techniques are needed in order to minimize the risk of inducing seismicity in geologic carbon storage projects.

10   **8. MINIMIZING THE RISK OF INDUCING FELT SEISMICITY**

To effectively minimize the risk of inducing large earthquakes that are felt on the ground surface and may damage structures, the following steps should be followed:

1) performing a detailed initial site characterization, including the determination of:

- the geomechanical properties (Young's modulus, Poisson ratio, cohesion and
15   friction angle) of the geological formations relevant to the site (at least of the storage formation, the caprock and base rock);

- the hydraulic properties (permeability and porosity) of the geological formations relevant to the site (at least of the storage formation, the caprock and base rock);

- the thermal properties (thermal conductivity and heat capacity) of the geological
20   formations relevant to the site (at least of the storage formation, the caprock and base rock);

- the seismic velocities v_p and v_s from the surface to the crystalline basement. An accurate determination of these velocities is important to locate the hypocenters of the induced seismicity with precision;

- the baseline of natural seismicity to establish the initial a and b values of the Gutenberg-Richter law in order to discriminate induced from natural seismicity;

- the initial pressure, temperature and stresses profiles with depth from the surface to the crystalline basement. The determination of the stress state is particularly important to perform a fault stability analysis of the identified faults and determining the strike and dip of critically oriented faults;

- characteristics of geological formations and faults and their location and orientation through 3D seismic data;

2) putting in place proper monitoring for performing continuous characterization, including:

- an array of geophones at depth to measure and locate induced microseismicity;

- a network of geophones on surface or in shallow wells with adequate spatial distribution, covering the whole footprint of the storage site to accurately locate induce seismicity. Induced events should be located in quasi-real time, together with their focal mechanisms to detect potentially unidentified faults that may induce large earthquakes. Inversion of the stress tensor is also important to detect possible rotations (Martinez-Garzon et al., 2013, 2014), which could be induced by pressure buildup, cooling and/or shear slip stress transfer (De Simone et al., 2017). This seismic continuous characterization is particularly important when CO_2 is injected in the basal aquifer (Verdon, 2014; Will et al., 2016);

- monitoring wells measuring pressure, temperature and CO_2 saturation in the storage formation, caprock and secondary aquifer above the storage formation. Monitoring in secondary aquifers is useful for detecting brine and CO_2 leakage (e.g., Chabora and Benson, 2009; Zeidouni et al., 2014). Pressure measurements

can be used for a continuous characterization technique as the one described in Section 7;

3) carrying out pressure management:

- based on the thermo-hydro-mechanical-seismic (THMS) monitoring and characterization, predictive models of induced seismicity that consider coupled THMS processes should be applied to identify the injection scenario that minimizes future induced seismicity. The continuous characterization will permit updating the fault stability analysis by incorporating newly detected faults. The range (taking into account the uncertainty on faults properties) of pressure buildup that makes faults become critically oriented for shear failure can be determined from the initial stress state, the strike and dip of faults, and the stress changes induced by CO_2 injection. Pressure management should be applied to avoid exceeded hazardous levels of pressure buildup around faults. To limit pressure, the injection rate may need to be lowered or pressure may need to be released in the vicinity of critically oriented faults (Birkholzer et al., 2012);

- storage alternatives to the conventional concept of storing CO_2 in deep saline aquifers may be used to have a better control on pressure buildup. For example, injection of CO_2 dissolved into brine is achieved by creating dipoles of wells in which brine is extracted from the storage formation and reinjected together with CO_2 in the same formation (Burton and Bryant, 2009; Jain and Bryant, 2011; Pool et al., 2013). The dipoles of wells limit pressure buildup and allow to have a better control on it. Similarly, geothermal energy production using CO_2 as a working fluid permits lowering pressure buildup and additionally extract geothermal energy (Randolph and Saar, 2011). Despite the promising potential of this technology, the only pilot site that has tried CO_2 as a working fluid yielded

a low performance because the thermosyphon that should permit circulating CO_2 with a negligible energy consumption was not formed properly (Freifeld et al., 2016). Nevertheless, future research should enable a successful deployment of this technology.

9. CONCLUSIONS

Geologic carbon storage can successfully store gigatone scale of CO_2 at a low level of induced seismicity provided that proper site characterization, monitoring and pressure management are performed. There are several factors that favor the low induce seismicity risk. First, sedimentary formations where CO_2 is planned to be stored are, in general, not critically stressed, which permits generating a certain pressure buildup without reaching shear failure conditions. Special care should be taken if CO_2 is injected in the basal aquifer, because the crystalline basement is critically stressed and may contain unidentified faults that are critically oriented for shear slip. Additionally, CO_2 pressure evolution is relatively easy to control because pressure stabilizes after an initial sharp pressure buildup, becoming practically constant. Despite this favorable pressure evolution, if low-permeable faults are present, an additional pressure buildup may cause large stress changes in the fault, leading to its reactivation. To prevent this situation, a detailed site characterization, both before the start of operation of projects and continuously during the whole operational stage, monitoring and pressure management should permit minimizing the risk of inducing large (felt) earthquakes.

ACKNOWLEDGEMENTS

VV acknowledges funding from the European Research Council (ERC) under the
European Union's Horizon 2020 research and innovation programme (grant agreement
No. 801809). JR acknowledges funding by the Assistant Secretary for Fossil Energy,

5   National Energy Technology Laboratory, National Risk Assessment Partnership of the
U.S. Department of Energy to the Lawrence Berkeley National Laboratory under
Contract No. DEAC02-05CH11231.

REFERENCES

10   Alcalde, J., Martí, D., Calahorrano, A., Marzán, I., Ayarza, P., Carbonell, R., Juhlin, C.
and Pérez-Estaún, A.: Active seismic characterization experiments of the Hontomín
research facility for geological storage of CO_2, Spain, International Journal of
Greenhouse Gas Control, 19, 785-795, https://doi.org/10.1016/j.ijggc.2013.01.039,
2013.

15   Alcalde, J., Marzán, I., Saura, E., Martí, D., Ayarza, P., Juhlin, C., Pérez-Estaún, A. and
Carbonell, R.: 3D geological characterization of the Hontomín CO_2 storage site, Spain:
Multidisciplinary approach from seismic, well-log and regional data, Tectonophysics,
627, 6-25, https://doi.org/10.1016/j.tecto.2014.04.025, 2014.

Bakker, E., Hangx, S. J., Niemeijer, A. R. and Spiers, C. J.: Frictional behaviour and
20   transport properties of simulated fault gouges derived from a natural CO_2 reservoir,
International Journal of Greenhouse Gas Control, 54, 70-83,
https://doi.org/10.1016/j.ijggc.2016.08.029, 2016.

Bao, J., Xu, Z. and Fang, Y.: A coupled thermal-hydro-mechanical simulation for carbon
dioxide sequestration, Environ. Geotechnics, paper 14.00002,
25   http://dx.doi.org/10.1680/envgeo.14.00002, 2014.

Bauer, R. A., Carney, M. and Finley, R. J.: Overview of microseismic response to CO_2
injection into the Mt. Simon saline reservoir at the Illinois Basin-Decatur Project,
International Journal of Greenhouse Gas Control, 54, 378-388,
https://doi.org/10.1016/j.ijggc.2015.12.015, 2016.

30   Benson, S. M. and Cole, D. R.: CO_2 sequestration in deep sedimentary formations,
Elements, 4(5), 325-331, https://doi.org/10.2113/gselements.4.5.325, 2008.

Birkholzer, J. T., Cihan, A. and Zhou, Q.: Impact-driven pressure management via
targeted brine extraction—Conceptual studies of CO_2 storage in saline formations,
International Journal of Greenhouse Gas Control, 7, 168-180,
35   https://doi.org/10.1016/j.ijggc.2012.01.001, 2012.

Bourdet, D., Whittle, T. M., Douglas, A. A. and Pirard, Y. M.: A new set of type curves
simplifies well test analysis, World Oil, 196(6), 95-106, 1983.

Burton, M. and Bryant, S. L.: Surface dissolution: minimizing groundwater impact and leakage risk simultaneously, Energy Procedia, 1(1), 3707-3714, https://doi.org/10.1016/j.egypro.2009.02.169, 2009.

5 Buscheck, T. A., Sun, Y., Chen, M., Hao, Y., Wolery, T. J., Bourcier, W. L., Court, B., Celia, M.A., Friedman, J. and Aines, R. D.: Active CO_2 reservoir management for carbon storage: Analysis of operational strategies to relieve pressure buildup and improve injectivity, International Journal of Greenhouse Gas Control, 6, 230-245, https://doi.org/10.1016/j.ijggc.2011.11.007, 2012.

Butler, J. J. and Liu, W.: Pumping tests in nonuniform aquifers: The radially asymmetric

10 case, Water Resources Research, 29(2), 259-269, https://doi.org/10.1029/92WR02128, 1993.

Cai, M., Morioka, H., Kaiser, P. K., Tasaka, Y., Kurose, H., Minami, M. and Maejima, T.: Back-analysis of rock mass strength parameters using AE monitoring data. International Journal of Rock Mechanics and Mining Sciences, 44(4), 538-549,

15 https://doi.org/10.1016/j.ijrmms.2006.09.012, 2007.

Caine, J. S., Evans, J. P. and Forster, C. B.: Fault zone architecture and permeability structure, Geology, 24(11), 1025-1028, https://doi.org/10.1130/0091-7613(1996)024<1025:FZAAPS>2.3.CO;2 , 1996.

Cappa, F. and Rutqvist, J.: Impact of CO_2 geological sequestration on the nucleation of

20 earthquakes, Geophysical Research Letters, 38(17), L17313, https://doi.org/10.1029/2011GL048487, 2011a.

Cappa, F. and Rutqvist, J.: Modeling of coupled deformation and permeability evolution during fault reactivation induced by deep underground injection of CO_2, International Journal of Greenhouse Gas Control, 5(2), 336-346,

25 https://doi.org/10.1016/j.ijggc.2010.08.005, 2011b.

Castelletto, N., Teatini, P., Gambolati, G., Bossie-Codreanu, D., Vincké, O., Daniel, J. M., Battistelli, A., Marcolini, M., Donde, F. and Volpi, V.: Multiphysics modeling of CO_2 sequestration in a faulted saline formation in Italy, Advances in Water Resources, 62, 570-587, https://doi.org/10.1016/j.advwatres.2013.04.006, 2013a.

30 Castelletto, N., Gambolati, G. and Teatini, P.: Geological CO_2 sequestration in multi-compartment reservoirs: Geomechanical challenges, Journal of Geophysical Research: Solid Earth, 118(5), 2417-2428, https://doi.org/10.1002/jgrb.50180, 2013b.

Celia, M. A.: Geological storage of captured carbon dioxide as a large-scale carbon mitigation option, Water Resources Research, 53(5), 3527-3533,

35 https://doi.org/10.1002/2017WR020841, 2017.

Cesca, S., Grigoli, F., Heimann, S., González, A., Buforn, E., Maghsoudi, S., Blancg, E. and Dahm, T.: The 2013 September–October seismic sequence offshore Spain: a case of seismicity triggered by gas injection?, Geophysical Journal International, 198(2), 941-953, https://doi.org/10.1093/gji/ggu172, 2014.

40 Chabora, E. R. and Benson, S. M.: Brine displacement and leakage detection using pressure measurements in aquifers overlying CO_2 storage reservoirs, Energy Procedia, 1(1), 2405-2412, https://doi.org/10.1016/j.egypro.2009.01.313, 2009.

Chen, F., Wiese, B., Zhou, Q., Kowalsky, M. B., Norden, B., Kempka, T. and Birkholzer, J. T.: Numerical modeling of the pumping tests at the Ketzin pilot site for CO_2

45 injection: Model calibration and heterogeneity effects, International Journal of Greenhouse Gas Control, 22, 200-212, https://doi.org/10.1016/j.ijggc.2014.01.003, 2014.

Chiaramonte, L., White, J. A. and Trainor-Guitton, W.: Probabilistic geomechanical analysis of compartmentalization at the Snøhvit CO_2 sequestration project, Journal of Geophysical Research: Solid Earth, 120(2), 1195-1209, https://doi.org/10.1002/2014JB011376, 2015.

5   Clarke, H., Eisner, L., Styles, P. and Turner, P.: Felt seismicity associated with shale gas hydraulic fracturing: The first documented example in Europe, Geophysical Research Letters, 41(23), 8308-8314, https://doi.org/10.1002/2014GL062047, 2014.

Cooper, H. H. and Jacob, C. E.: A generalized graphical method for evaluating formation constants and summarizing well-field history, Eos, Transactions American
10   Geophysical Union, 27(4), 526-534, https://doi.org/10.1029/TR027i004p00526, 1946.

Cornet, F. H. and Jianmin, Y.: Analysis of induced seismicity for stress field determination and pore pressure mapping. In Mechanics Problems in Geodynamics Part I (pp. 677-700). Birkhäuser Basel, https://doi.org/10.1007/978-3-0348-9065-6_16, 1995.

15   Cornet F.H., Helm J., Poitrenaud H. and Etchecopar A.: Seismic and Aseismic Slips Induced by Large-scale Fluid Injections. In: Talebi S. (eds) Seismicity Associated with Mines, Reservoirs and Fluid Injections. Pageoph Topical Volumes. Birkhäuser, Basel, https://doi.org/10.1007/978-3-0348-8814-1_12, 1997.

De Simone, S., Carrera, J. and Vilarrasa, V.: Superposition approach to understand
20   triggering mechanisms of post-injection induced seismicity, Geothermics, 70, 85-97, https://doi.org/10.1016/j.geothermics.2017.05.011, 2017.

Deichmann, N. and Giardini, D.: Earthquakes induced by the stimulation of an enhanced geothermal system below Basel (Switzerland), Seismological Research Letters, 80(5), 784-798, https://doi.org/10.1785/gssrl.80.5.784 , 2009.

25   Deichmann, N., Kraft, T. and Evans, K. F.: Identification of faults activated during the stimulation of the Basel geothermal project from cluster analysis and focal mechanisms of the larger magnitude events, Geothermics, 52, 84-97, https://doi.org/10.1016/j.geothermics.2014.04.001, 2014.

Dempsey, D., Kelkar, S. and Pawar, R.: Passive injection: A strategy for mitigating
30   reservoir pressurization, induced seismicity and brine migration in geologic CO_2 storage, International Journal of Greenhouse Gas Control, 28, 96-113, https://doi.org/10.1016/j.ijggc.2014.06.002, 2014.

Diehl, T., Kraft, T., Kissling, E. and Wiemer, S.: The induced earthquake sequence related to the St. Gallen deep geothermal project (Switzerland): Fault reactivation and fluid
35   interactions imaged by microseismicity, Journal of Geophysical Research: Solid Earth, 122(9), 7272-7290, https://doi.org/10.1002/2017JB014473, 2017.

Edwards, B., Kraft, T., Cauzzi, C., Kästli, P. and Wiemer, S.: Seismic monitoring and analysis of deep geothermal projects in St Gallen and Basel, Switzerland, Geophysical Journal International, 201(2), 1022-1039, https://doi.org/10.1093/gji/ggv059, 2015.

40   Egholm, D. L., Clausen, O. R., Sandiford, M., Kristensen, M. B. and Korstgård, J. A.: The mechanics of clay smearing along faults, Geology, 36(10), 787-790, https://doi.org/10.1130/G24975A.1 , 2008.

Ellsworth, W. L.: Injection-induced earthquakes, Science, 341(6142), 1225942, DOI: 10.1126/science.1225942, 2013.

45   Evans, K. F., Moriya, H., Niitsuma, H., Jones, R. H., Phillips, W. S., Genter, A., Sausse, J., Jung, R. and Baria, R.: Microseismicity and permeability enhancement of hydrogeologic structures during massive fluid injections into granite at 3 km depth at

the Soultz HDR site, Geophysical Journal International, 160(1), 388-412, https://doi.org/10.1111/j.1365-246X.2004.02474.x, 2005.

Faulkner, D. R., Mitchell, T. M., Healy, D. and Heap, M. J.: Slip on 'weak' faults by the rotation of regional stress in the fracture damage zone, Nature, 444(7121), 922-925, https://doi.org/10.1038/nature05353, 2006.

Figueiredo, B., Tsang, C. F., Rutqvist, J., Bensabat, J. and Niemi, A.: Coupled hydro-mechanical processes and fault reactivation induced by CO_2 injection in a three-layer storage formation, International Journal of Greenhouse Gas Control, 39, 432-448, https://doi.org/10.1016/j.ijggc.2015.06.008, 2015.

Freifeld, B. M., Pan, L., Doughty, C., Zakem, S., Hart, K. and Hostler, S.: Demonstration of Geothermal Energy Production Using Carbon Dioxide as a Working Fluid at the SECARB Cranfield Site, Cranfield, Mississippi. In Proceedings of the forty-first workshop on geothermal reservoir engineering, Stanford University, 2016.

Gaite, B., Ugalde, A., Villaseñor, A. and Blanch, E.: Improving the location of induced earthquakes associated with an underground gas storage in the Gulf of Valencia (Spain), Physics of the Earth and Planetary Interiors, 254, 46-59, https://doi.org/10.1016/j.pepi.2016.03.006, 2016.

Gilfillan, S. M., Lollar, B. S., Holland, G., Blagburn, D., Stevens, S., Schoell, M., ... & Ballentine, C. J.: Solubility trapping in formation water as dominant CO_2 sink in natural gas fields, Nature, 458(7238), 614, https://doi.org/10.1038/nature07852, 2009.

Goodarzi, S., Settari, A., Zoback, M. D. and Keith, D.: Thermal aspects of geomechanics and induced fracturing in CO_2 injection with application to CO_2 sequestration in Ohio River Valley. In SPE International Conference on CO_2 Capture, Storage, and Utilization. Society of Petroleum Engineers, https://doi.org/10.2118/139706-MS, 2010.

Goodarzi, S., Settari, A. and Keith, D.: Geomechanical modeling for CO_2 storage in Nisku aquifer in Wabamun Lake area in Canada, International Journal of Greenhouse Gas Control, 10, 113-122, https://doi.org/10.1016/j.ijggc.2012.05.020, 2012.

Goodarzi, S., Settari, A., Zoback, M. D. and Keith, D. W.: Optimization of a CO_2 storage project based on thermal, geomechanical and induced fracturing effects, Journal of Petroleum Science and Engineering, 134, 49-59, https://doi.org/10.1016/j.petrol.2015.06.004, 2015.

Gor, G. Y., Elliot, T. R. and Prévost, J. H.: Effects of thermal stresses on caprock integrity during CO_2 storage, International Journal of Greenhouse Gas Control, 12, 300-309, https://doi.org/10.1016/j.ijggc.2012.11.020, 2013.

Grigoli, F., Cesca, S., Priolo, E., Rinaldi, A. P., Clinton, J. F., Stabile, T. A., Dost, B., Garcia Fernandez, M., Wiemer, S. and Dahm, T.: Current challenges in monitoring, discrimination, and management of induced seismicity related to underground industrial activities: A European perspective, Reviews of Geophysics, 55(2), 310-340, https://doi.org/10.1002/2016RG000542, 2017.

Guglielmi, Y., Cappa, F., Avouac, J. P., Henry, P. and Elsworth, D.: Seismicity triggered by fluid injection–induced aseismic slip, Science, 348(6240), 1224-1226, DOI: 10.1126/science.aab0476, 2015.

Hansen, O., Gilding, D., Nazarian, B., Osdal, B., Ringrose, P., Kristoffersen, J. B., Eiken, O. and Hansen, H.: Snøhvit: The history of injecting and storing 1 Mt CO_2 in the fluvial Tubåen Fm, Energy Procedia, 37, 3565-3573, https://doi.org/10.1016/j.egypro.2013.06.249, 2013.

Hantush, M. S.: Analysis of data from pumping tests in leaky aquifers, Eos, Transactions American Geophysical Union, 37(6), 702-714, https://doi.org/10.1029/TR037i006p00702, 1956.

Häring, M. O., Schanz, U., Ladner, F. and Dyer, B. C.: Characterisation of the Basel 1 enhanced geothermal system, Geothermics, 37(5), 469-495, https://doi.org/10.1016/j.geothermics.2008.06.002, 2008.

Henninges, J., Liebscher, A., Bannach, A., Brandt, W., Hurter, S., Köhler, S., Möller, F. and CO2SINK Group: PT-ρ and two-phase fluid conditions with inverted density profile in observation wells at the CO_2 storage site at Ketzin (Germany), Energy Procedia, 4, 6085-6090, https://doi.org/10.1016/j.egypro.2011.02.614, 2011.

Hidalgo, J. J. and Carrera, J.: Effect of dispersion on the onset of convection during CO_2 sequestration, Journal of Fluid Mechanics, 640, 441-452, https://doi.org/10.1017/S0022112009991480, 2009.

Hitchon, B., Gunter, W. D., Gentzis, T. and Bailey, R. T.: Sedimentary basins and greenhouse gases: a serendipitous association, Energy Conversion and Management, 40(8), 825-843, https://doi.org/10.1016/S0196-8904(98)00146-0, 1999.

Hsieh, P. A. and Bredehoeft, J. D.: A reservoir analysis of the Denver earthquakes: A case of induced seismicity, Journal of Geophysical Research: Solid Earth, 86(B2), 903-920, https://doi.org/10.1029/JB086iB02p00903, 1981.

Hsieh, P. A.: Deformation-induced changes in hydraulic head during ground-water withdrawal, Groundwater, 34(6), 1082-1089, https://doi.org/10.1111/j.1745-6584.1996.tb02174.x, 1996.

IPCC: Special report on Global warming of 1.5 ºC, 2018.

Jaeger, J. C., Cook, N. G. and Zimmerman, R.: Fundamentals of rock mechanics. John Wiley & Sons, 2009.

Jain, L. and Bryant, S. L.: Optimal design of injection/extraction wells for the surface dissolution CO_2 storage strategy, Energy Procedia, 4, 4299-4306, https://doi.org/10.1016/j.egypro.2011.02.380, 2011.

Jeanne, P., Rutqvist, J., Dobson, P. F., Walters, M., Hartline, C. and Garcia, J.: The impacts of mechanical stress transfers caused by hydromechanical and thermal processes on fault stability during hydraulic stimulation in a deep geothermal reservoir, International Journal of Rock Mechanics and Mining Sciences, 72, 149-163, https://doi.org/10.1016/j.ijrmms.2014.09.005, 2014.

Kaven, J. O., Hickman, S. H., McGarr, A. F. and Ellsworth, W. L.: Surface monitoring of microseismicity at the Decatur, Illinois, CO_2 sequestration demonstration site, Seismological Research Letters, 86(4), 1096-1101, https://doi.org/10.1785/0220150062, 2015.

Kim, S. and Hosseini, S. A.: Geological CO_2 storage: Incorporation of pore-pressure/stress coupling and thermal effects to determine maximum sustainable pressure limit, Energy Procedia, 63, 3339-3346, https://doi.org/10.1016/j.egypro.2014.11.362, 2014.

Kim, S. and Hosseini, S. A.: Hydro-thermo-mechanical analysis during injection of cold fluid into a geologic formation, International Journal of Rock Mechanics and Mining Sciences, 77, 220-236, https://doi.org/10.1016/j.ijrmms.2015.04.010, 2015.

King, G. C., Stein, R. S. and Lin, J.: Static stress changes and the triggering of earthquakes, Bulletin of the Seismological Society of America, 84(3), 935-953, 1994.

LaForce, T., Ennis-King, J. and Paterson, L.: Semi-analytical temperature and stress profiles for nonisothermal CO_2 injection. In Proceedings of the World Geothermal Congress, Melbourne, Australia, 19–25 April 2015, 2015.

Ledesma, A., Gens, A. and Alonso, E. E.: Parameter and variance estimation in geotechnical backanalysis using prior information, International Journal for Numerical and Analytical Methods in Geomechanics, 20(2), 119-141,

https://doi.org/10.1002/(SICI)1096-9853(199602)20:2<119::AID-NAG810>3.0.CO;2-L, 1996.

Lu, M. and Connell, L. D.: Non-isothermal flow of carbon dioxide in injection wells during geological storage, International Journal of Greenhouse Gas Control, 2(2), 248-258, https://doi.org/10.1016/S1750-5836(07)00114-4, 2008.

Luo, Z. and Bryant, S. L.: Influence of thermo-elastic stress on CO_2 injection induced fractures during storage, In SPE International Conference on CO_2 capture, storage, and utilization. Society of Petroleum Engineers, https://doi.org/10.2118/139719-MS, 2010.

Martínez-Garzón, P., Bohnhoff, M., Kwiatek, G. and Dresen, G.: Stress tensor changes related to fluid injection at The Geysers geothermal field, California, Geophysical Research Letters, 40(11), 2596-2601, https://doi.org/10.1002/grl.50438, 2013.

Martínez-Garzón, P., Kwiatek, G., Ickrath, M. and Bohnhoff, M.: MSATSI: A MATLAB package for stress inversion combining solid classic methodology, a new simplified user-handling, and a visualization tool, Seismological Research Letters, 85(4), 896-904, https://doi.org/10.1785/0220130189 , 2014.

Mathias, S. A., Gluyas, J. G., González Martínez de Miguel, G. J. and Hosseini, S. A.: Role of partial miscibility on pressure buildup due to constant rate injection of CO_2 into closed and open brine aquifers, Water Resources Research, 47(12), https://doi.org/10.1029/2011WR011051, 2011a.

Mathias, S. A., Gonzalez Martinez de Miguel, G. J., Thatcher, K. E. and Zimmerman, R. W.; Pressure buildup during CO_2 injection into a closed brine aquifer, Transport in Porous Media, 89(3), 383-397, https://doi.org/10.1007/s11242-011-9776-z, 2011b.

Morris, A., Ferrill, D. A. and Henderson, D. B.: Slip-tendency analysis and fault reactivation, Geology, 24(3), 275-278, https://doi.org/10.1130/0091-7613(1996)024<0275:STAAFR>2.3.CO;2 , 1996.

Myer, L. R. and Daley, T. M.: Elements of a best practices approach to induced seismicity in geologic storage, Energy Procedia, 4, 3707-3713, https://doi.org/10.1016/j.egypro.2011.02.303, 2011.

Neuzil, C. E.: How permeable are clays and shales?, Water Resources Research, 30(2), 145-150, https://doi.org/10.1029/93WR02930, 1994.

Niemi, A., Edlmann, K., Carrera, J., Juhlin, C., Tatomir, A., Ghergut, I., Sauter, M., Bensabat, J., Fagerlund, F., Rasmusson, K., Cornet, F. H., McDermott, C. I. and Vilarrasa, V.: Site Characterization. In Geological Storage of CO_2 in Deep Saline Formations, pp. 309-380, Springer, Dordrecht, DOI 10.1007/978-94-024-0996-3_7, 2017.

Okada, Y.: Internal deformation due to shear and tensile faults in a half-space, Bulletin of the Seismological Society of America, 82(2), 1018-1040, 1992.

Okwen, R. T., Stewart, M. T. and Cunningham, J. A.: Temporal variations in near-wellbore pressures during CO_2 injection in saline aquifers, International Journal of Greenhouse Gas Control, 5(5), 1140-1148, https://doi.org/10.1016/j.ijggc.2011.07.011, 2011.

Oldenburg, C. M.: The risk of induced seismicity: is cap-rock integrity on shaky ground?, Greenhouse Gases: Science and Technology, 2(4), 217-8, DOI 10/1002/ghg.1299, 2012.

Parotidis, M., Shapiro, S. A. and Rothert, E.: Back front of seismicity induced after termination of borehole fluid injection, Geophysical Research Letters, 31(2), L02612, https://doi.org/10.1029/2003GL018987, 2004.

Paterson, L., Lu, M., Connell, L.D. and Ennis-King, J.: Numerical modeling of pressure and temperature profiles including phase transitions in carbon dioxide wells, SPE Annual Technical Conference and Exhibition, Denver, 21-24 September 2008, https://doi.org/10.2118/115946-MS, 2008.

Pau, G. S., Bell, J. B., Pruess, K., Almgren, A. S., Lijewski, M. J. and Zhang, K.: High-resolution simulation and characterization of density-driven flow in CO_2 storage in saline aquifers, Advances in Water Resources, 33(4), 443-455, https://doi.org/10.1016/j.advwatres.2010.01.009, 2010.

Pereira, L. C., Guimarães, L. J., Horowitz, B. and Sánchez, M.: Coupled hydro-mechanical fault reactivation analysis incorporating evidence theory for uncertainty quantification, Computers and Geotechnics, 56, 202-215, https://doi.org/10.1016/j.compgeo.2013.12.007, 2014.

Pool, M., Carrera, J., Vilarrasa, V., Silva, O. and Ayora, C.: Dynamics and design of systems for geological storage of dissolved CO_2, Advances in Water Resources, 62, 533-542, https://doi.org/10.1016/j.advwatres.2013.10.001, 2013.

Pruess, K.: Enhanced geothermal systems (EGS) using CO_2 as working fluid—A novel approach for generating renewable energy with simultaneous sequestration of carbon, Geothermics, 35(4), 351-367, https://doi.org/10.1016/j.geothermics.2006.08.002, 2006.

Randolph, J. B. and Saar, M. O.: Combining geothermal energy capture with geologic carbon dioxide sequestration, Geophysical Research Letters, 38(10), L10401, https://doi.org/10.1029/2011GL047265, 2011.

Renard, P., Glenz, D. and Mejias, M.: Understanding diagnostic plots for well-test interpretation, Hydrogeology Journal, 17(3), 589-600, https://doi.org/10.1007/s10040-008-0392-0, 2009.

Riaz, A., Hesse, M., Tchelepi, H. A. and Orr, F. M.: Onset of convection in a gravitationally unstable diffusive boundary layer in porous media, Journal of Fluid Mechanics, 548, 87-111, https://doi.org/10.1017/S0022112005007494, 2006.

Rinaldi, A. P. and Rutqvist, J.: Modeling of deep fracture zone opening and transient ground surface uplift at KB-502 CO_2 injection well, In Salah, Algeria, International Journal of Greenhouse Gas Control, 12, 155-167, https://doi.org/10.1016/j.ijggc.2012.10.017, 2013.

Rinaldi, A. P., Jeanne, P., Rutqvist, J., Cappa, F. and Guglielmi, Y.: Effects of fault-zone architecture on earthquake magnitude and gas leakage related to CO_2 injection in a multi-layered sedimentary system, Greenhouse Gases: Science and Technology, 4(1), 99-120, https://doi.org/10.1002/ghg.1403, 2014.

Rinaldi, A. P., Vilarrasa, V., Rutqvist, J. and Cappa, F.: Fault reactivation during CO_2 sequestration: Effects of well orientation on seismicity and leakage, Greenhouse Gases: Science and Technology, 5(5), 645-656, https://doi.org/10.1002/ghg.1511, 2015.

Rohmer, J., Pluymakers, A. and Renard, F.: Mechano-chemical interactions in sedimentary rocks in the context of CO_2 storage: Weak acid, weak effects?, Earth-Science Reviews, 157, 86-110, https://doi.org/10.1016/j.earscirev.2016.03.009, 2016.

Rubinstein, J. L. and Mahani, A. B.: Myths and facts on wastewater injection, hydraulic fracturing, enhanced oil recovery, and induced seismicity, Seismological Research Letters, 86(4), 1060-1067, https://doi.org/10.1785/0220150067 , 2015.

Rutqvist, J., Birkholzer, J., Cappa, F. and Tsang, C. F.: Estimating maximum sustainable injection pressure during geological sequestration of CO_2 using coupled fluid flow and geomechanical fault-slip analysis, Energy Conversion and Management, 48(6), 1798-1807, https://doi.org/10.1016/j.enconman.2007.01.021, 2007.

Rutqvist, J.: The geomechanics of CO_2 storage in deep sedimentary formations, Geotechnical and Geological Engineering, 30(3), 525-551, https://doi.org/10.1007/s10706-011-9491-0, 2012.

Rutqvist, J.: Fractured rock stress-permeability relationships from in situ data and effects of temperature and chemical-mechanical couplings, Geofluids, 15(1-2), 48-66, https://doi.org/10.1111/gfl.12089, 2015.

Rutqvist, J., Rinaldi, A. P., Cappa, F., Jeanne, P., Mazzoldi, A., Urpi, L., Guglielmi, Y. and Vilarrasa, V.: Fault activation and induced seismicity in geological carbon storage–Lessons learned from recent modeling studies, Journal of Rock Mechanics and Geotechnical Engineering, 8(6), 789-804, https://doi.org/10.1016/j.jrmge.2016.09.001, 2016.

Shapiro, S. A., Rothert, E., Rath, V. and Rindschwentner, J.: Characterization of fluid transport properties of reservoirs using induced microseismicity, Geophysics, 67(1), 212-220, https://doi.org/10.1190/1.1451597, 2002.

Steketee, J. A.: On Volterra's dislocations in a semi-infinite elastic medium, Canadian Journal of Physics, 36(2), 192-205, https://doi.org/10.1139/p58-024, 1958.

Stork, A. L., Verdon, J. P. and Kendall, J. M.: The microseismic response at the In Salah Carbon Capture and Storage (CCS) site, International Journal of Greenhouse Gas Control, 32, 159-171, https://doi.org/10.1016/j.ijggc.2014.11.014, 2015.

Streit, J. E. and Hillis, R. R.: Estimating fault stability and sustainable fluid pressures for underground storage of CO_2 in porous rock, Energy, 29(9-10), 1445-1456, https://doi.org/10.1016/j.energy.2004.03.078, 2004.

Szulczewski, M. L., MacMinn, C. W., Herzog, H. J. and Juanes, R.: Lifetime of carbon capture and storage as a climate-change mitigation technology, Proceedings of the National Academy of Sciences, 109(14), 5185-5189, https://doi.org/10.1073/pnas.1115347109, 2012.

Takahashi, M.: Permeability change during experimental fault smearing, Journal of Geophysical Research: Solid Earth, 108(B5), https://doi.org/10.1029/2002JB001984, 2003.

Theis, C. V.: The relation between the lowering of the piezometric surface and the rate and duration of discharge of a well using ground-water storage, Eos, Transactions American Geophysical Union, 16(2), 519-524, https://doi.org/10.1029/TR016i002p00519, 1935.

Vasco, D. W., Rucci, A., Ferretti, A., Novali, F., Bissell, R. C., Ringrose, P. S., Mathieson, A. S. and Wright, I. W.: Satellite-based measurements of surface deformation reveal fluid flow associated with the geological storage of carbon dioxide, Geophysical Research Letters, 37(3), L03303, https://doi.org/10.1029/2009GL041544, 2010.

Verdon, J. P., Kendall, J. M., White, D. J. and Angus, D. A.: Linking microseismic event observations with geomechanical models to minimise the risks of storing CO_2 in

geological formations, Earth and Planetary Science Letters, 305(1-2), 143-152, https://doi.org/10.1016/j.epsl.2011.02.048, 2011.

Verdon, J. P.: Significance for secure CO_2 storage of earthquakes induced by fluid injection, Environmental Research Letters, 9(6), 064022, https://doi.org/10.1088/1748-9326/9/6/064022, 2014.

Verdon, J. P., Stork, A. L., Bissell, R. C., Bond, C. E. and Werner, M. J.: Simulation of seismic events induced by CO_2 injection at In Salah, Algeria, Earth and Planetary Science Letters, 426, 118-129, https://doi.org/10.1016/j.epsl.2015.06.029, 2015.

Vidal-Gilbert, S., Tenthorey, E., Dewhurst, D., Ennis-King, J., Van Ruth, P. and Hillis, R.: Geomechanical analysis of the Naylor Field, Otway Basin, Australia: Implications for CO_2 injection and storage, International Journal of Greenhouse Gas Control, 4(5), 827-839, https://doi.org/10.1016/j.ijggc.2010.06.001, 2010.

Vilarrasa, V., Bolster, D., Olivella, S. and Carrera, J.: Coupled hydromechanical modeling of CO_2 sequestration in deep saline aquifers, International Journal of Greenhouse Gas Control, 4(6), 910-919, https://doi.org/10.1016/j.ijggc.2010.06.006, 2010.

Vilarrasa, V., Koyama, T., Neretnieks, I. and Jing, L.: Shear-induced flow channels in a single rock fracture and their effect on solute transport, Transport in Porous Media, 87(2), 503-523, https://doi.org/10.1007/s11242-010-9698-1, 2011.

Vilarrasa, V., Carrera, J., Bolster, D. and Dentz, M.: Semianalytical solution for CO_2 plume shape and pressure evolution during CO_2 injection in deep saline formations, Transport in Porous Media, 97(1), 43-65, https://doi.org/10.1007/s11242-012-0109-7, 2013a.

Vilarrasa, V., Silva, O., Carrera, J. and Olivella, S.: Liquid CO_2 injection for geological storage in deep saline aquifers, International Journal of Greenhouse Gas Control, 14, 84-96, https://doi.org/10.1016/j.ijggc.2013.01.015, 2013b.

Vilarrasa, V., Carrera, J. and Olivella, S.: Hydromechanical characterization of CO_2 injection sites, International Journal of Greenhouse Gas Control, 19, 665-677, https://doi.org/10.1016/j.ijggc.2012.11.014, 2013c.

Vilarrasa, V., Olivella, S., Carrera, J. and Rutqvist, J.: Long term impacts of cold CO_2 injection on the caprock integrity, International Journal of Greenhouse Gas Control, 24, 1-13, https://doi.org/10.1016/j.ijggc.2014.02.016, 2014.

Vilarrasa, V., Rutqvist, J. and Rinaldi, A. P.: Thermal and capillary effects on the caprock mechanical stability at In Salah, Algeria, Greenhouse Gases: Science and Technology, 5(4), 449-461, https://doi.org/10.1002/ghg.1486, 2015.

Vilarrasa, V. and Carrera, J.: Geologic carbon storage is unlikely to trigger large earthquakes and reactivate faults through which CO_2 could leak, Proceedings of the National Academy of Sciences, 112(19), 5938-5943, https://doi.org/10.1073/pnas.1413284112, 2015.

Vilarrasa, V. and Laloui, L.: Potential fracture propagation into the caprock induced by cold CO_2 injection in normal faulting stress regimes, Geomechanics for Energy and the Environment, 2, 22-31, https://doi.org/10.1016/j.gete.2015.05.001, 2015.

Vilarrasa, V.: The role of the stress regime on microseismicity induced by overpressure and cooling in geologic carbon storage, Geofluids, 16(5), 941-953, https://doi.org/10.1111/gfl.12197, 2016.

Vilarrasa, V., Makhnenko, R. and Gheibi, S.: Geomechanical analysis of the influence of CO_2 injection location on fault stability, Journal of Rock Mechanics and Geotechnical Engineering, 8(6), 805-818, https://doi.org/10.1016/j.jrmge.2016.06.006, 2016.

Vilarrasa, V. and Makhnenko, R. Y.: Caprock integrity and induced seismicity from laboratory and numerical experiments, Energy Procedia, 125, 494-503, https://doi.org/10.1016/j.egypro.2017.08.172, 2017.

Vilarrasa, V. and Rutqvist, J.: Thermal effects on geologic carbon storage, Earth-Science Reviews, 165, 245-256, https://doi.org/10.1016/j.earscirev.2016.12.011, 2017.

Vilarrasa, V., Rinaldi, A. P. and Rutqvist, J.: Long-term thermal effects on injectivity evolution during CO_2 storage, International Journal of Greenhouse Gas Control, 64, 314-322, https://doi.org/10.1016/j.ijggc.2017.07.019, 2017a.

Vilarrasa, V., Makhnenko, R. Y. and Laloui, L.: Potential for fault reactivation due to CO_2 injection in a semi-closed saline aquifer, Energy Procedia, 114, 3282-3290, https://doi.org/10.1016/j.egypro.2017.03.1460, 2017b.

Vilarrasa, V., Bustarret, G., Laloui, L. and Zeidouni, M.: A methodology to detect and locate low-permeability faults to reduce the risk of inducing seismicity of fluid injection operations in deep saline formations, International Journal of Greenhouse Gas Control, 59, 110-122, https://doi.org/10.1016/j.ijggc.2017.02.010, 2017c.

Wheatcraft, S. W. and Winterberg, F.: Steady state flow passing through a cylinder of permeability different from the surrounding medium, Water Resources Research, 21(12), 1923-1929, https://doi.org/10.1029/WR021i012p01923, 1985.

White, J. A. and Foxall, W.: Assessing induced seismicity risk at CO_2 storage projects: Recent progress and remaining challenges, International Journal of Greenhouse Gas Control, 49, 413-424, https://doi.org/10.1016/j.ijggc.2016.03.021, 2016.

Will, R., Smith, V., Lee, D. and Senel, O.: Data integration, reservoir response, and application, International Journal of Greenhouse Gas Control, 54, 389-403, https://doi.org/10.1016/j.ijggc.2015.12.020, 2016.

Yeo, I. W., De Freitas, M. H. and Zimmerman, R. W.: Effect of shear displacement on the aperture and permeability of a rock fracture, International Journal of Rock Mechanics and Mining Sciences, 35(8), 1051-1070, https://doi.org/10.1016/S0148-9062(98)00165-X, 1998.

Zareidarmiyan, A., Salarirad, H., Vilarrasa, V., De Simone, S. and Olivella, S.: Geomechanical response of fractured reservoirs, Fluids, 3(4), 70, doi:10.3390/fluids3040070, 2018.

Zeidouni, M., Nicot, J. P. and Hovorka, S. D.: Monitoring above-zone temperature variations associated with CO_2 and brine leakage from a storage aquifer, Environmental Earth Sciences, 72(5), 1733-1747, https://doi.org/10.1007/s12665-014-3077-0, 2014.

Zhang, L. Q., Yue, Z. Q., Yang, Z. F., Qi, J. X. and Liu, F. C.: A displacement-based back-analysis method for rock mass modulus and horizontal in situ stress in tunneling–Illustrated with a case study, Tunnelling and Underground Space Technology, 21(6), 636-649, https://doi.org/10.1016/j.tust.2005.12.001, 2006.

Zhou, Q., Birkholzer, J. T., Tsang, C. F. and Rutqvist, J.: A method for quick assessment of CO_2 storage capacity in closed and semi-closed saline formations, International Journal of Greenhouse Gas Control, 2(4), 626-639, https://doi.org/10.1016/j.ijggc.2008.02.004, 2008.
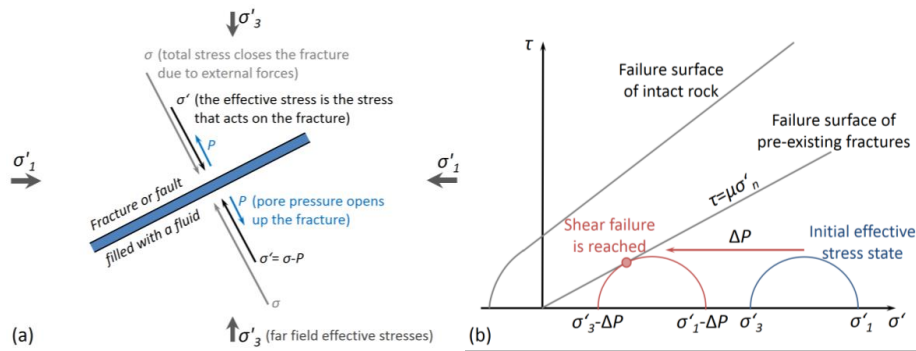
FIGURES

Figure 1: (a) Initial stress state of a fracture or fault of arbitrary orientation with respect to the far field effective stress and (b) Mohr circles showing how the reduction in effective stresses as a result of pressure buildup, ΔP, may induce shear failure in pre-existing fractures or faults. σ'_1 and σ'_3 are the maximum and minimum principal effective stresses, respectively, τ is tangential stress, σ'_n is normal effective stress to the fracture or fault, and μ is the friction coefficient.
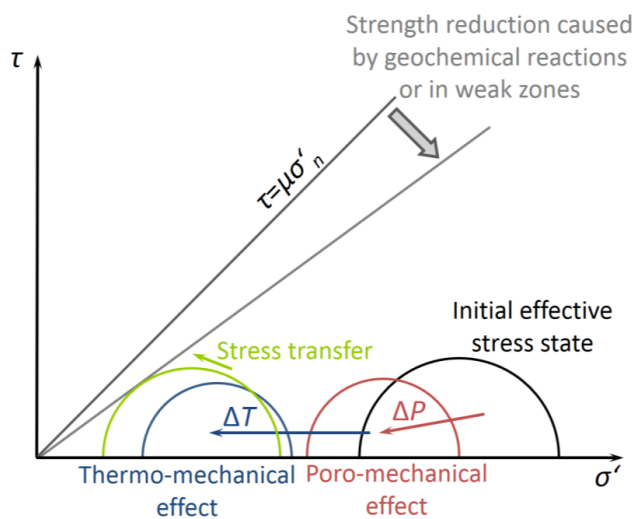
Figure 2: Schematic representation of several coupled effects on fracture/fault stability. Pressure buildup, ΔP, decreases the effective stresses and causes poro-mechanical stresses that change the size of the Mohr circle; temperature variations, ΔT, induce

5 thermal stresses; seismic and aseismic shear slip and interactions between geological layers with different rock properties produce total stress changes; and geochemical reactions may alter the strength of fractures and/or faults.
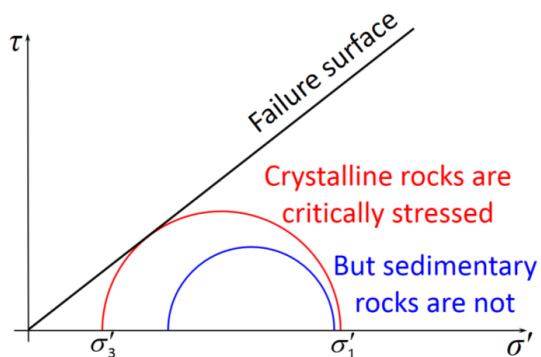
Figure 3: Stress state of crystalline and sedimentary rocks, showing that sedimentary rocks, which are the rocks where CO_2 will be stored, are usually not critically stressed.
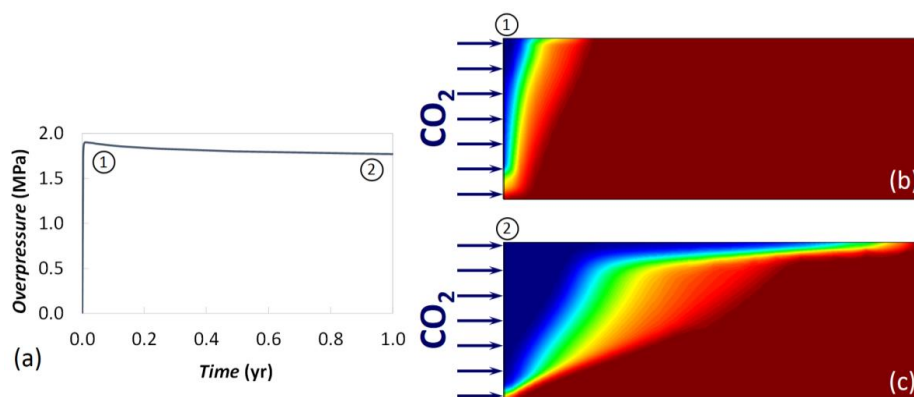
Figure 4: (a) CO_2 injection pressure evolution, (b) showing the CO_2 plume shape at the beginning of injection, coinciding with the peak in injection pressure (see number 1 in (a)), and (c) the CO_2 plume once gravity override dominates and the capillary fringe has been developed, leading to a slight pressure drop (see number 2 in (a)).
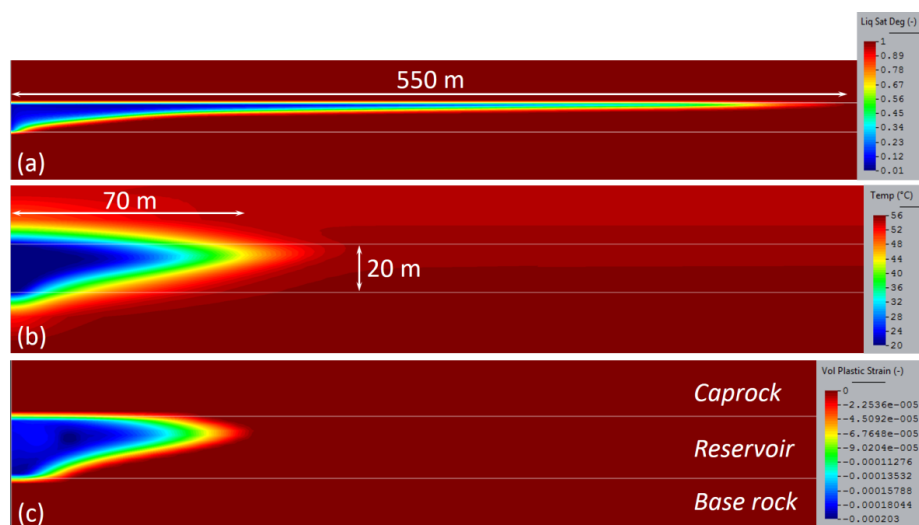
Figure 5: (a) Liquid saturation degree, (b) temperature distribution and (c) volumetric plastic strain after 2 years of injecting 1 Mt/yr of CO_2 through a vertical well. While (b) and (c) are plotted at the same scale, (a) is plotted at a smaller scale.
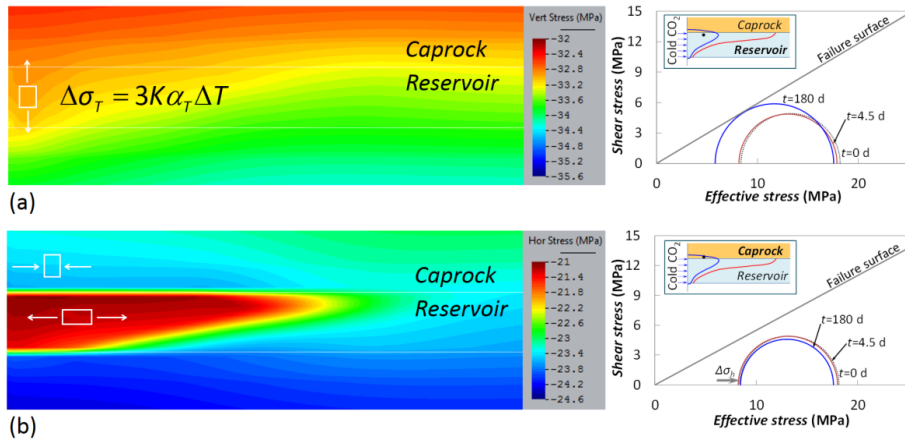
Figure 6: Total stresses in the (a) vertical and (b) horizontal direction after half a year of injecting 1 Mt/yr of CO_2 through a vertical well, indicating the sign of the induced stresses. Thermal stresses, $\Delta\sigma_T$, are proportional to the bulk modulus, K, the thermal expansion coefficient, α_T, and the temperature difference, ΔT. The change in the Mohr circles in (a) the reservoir and (b) the caprock is also represented.
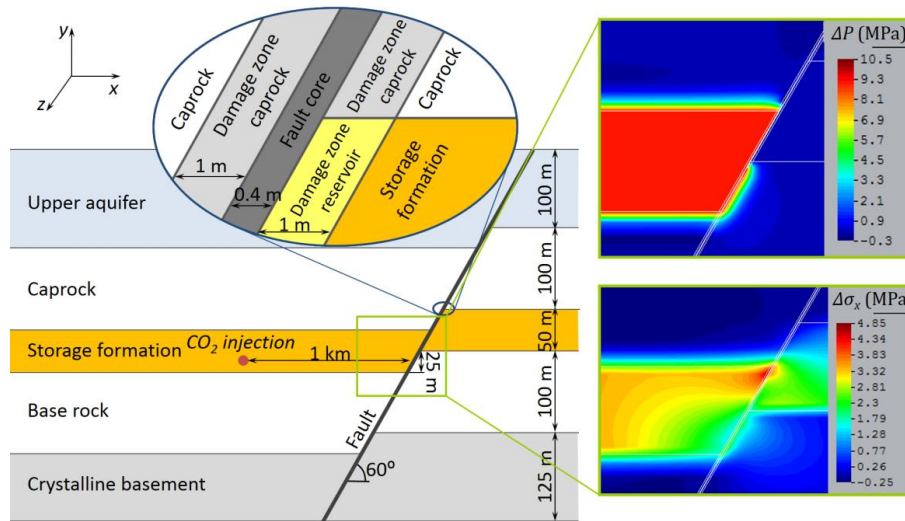
Figure 7: Geological setting in a normal faulting stress regime, including a low-permeable fault that leads to reservoir pressurization, ΔP, and horizontal stress changes in the in-plane direction, $\Delta\sigma_x$, when CO_2 is injected in the hanging wall for 1 year.
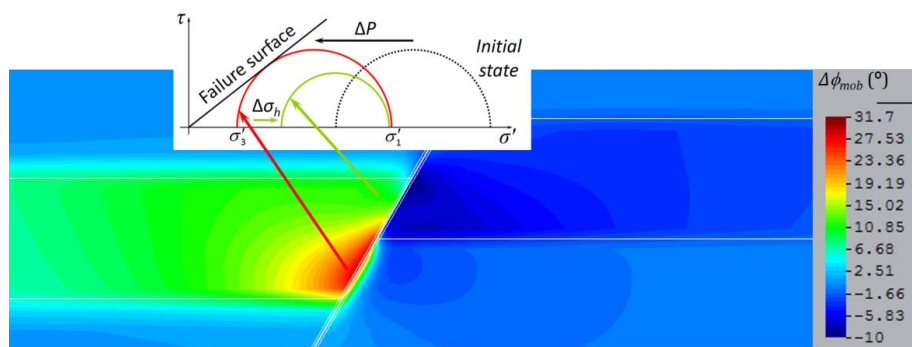
Figure 8: Distribution of stability changes induced by the pressure and stress changes shown in Figure 7, measured in terms of the mobilized friction angle, $\Delta\phi_{mob}$. The insert shows the Mohr circles before and after reservoir pressurization.
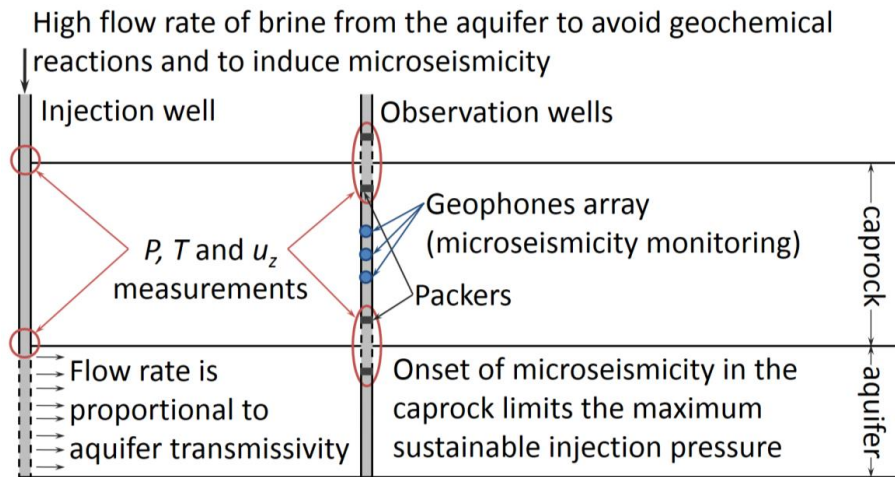
Figure 9: Hydro-mechanical characterization test proposed by Vilarrasa et al. (2013c) to quantify the rock properties at the field scale and obtain an initial estimate of the maximum sustainable injection pressure. P refers to pressure, T to temperature and u_z to vertical displacement.
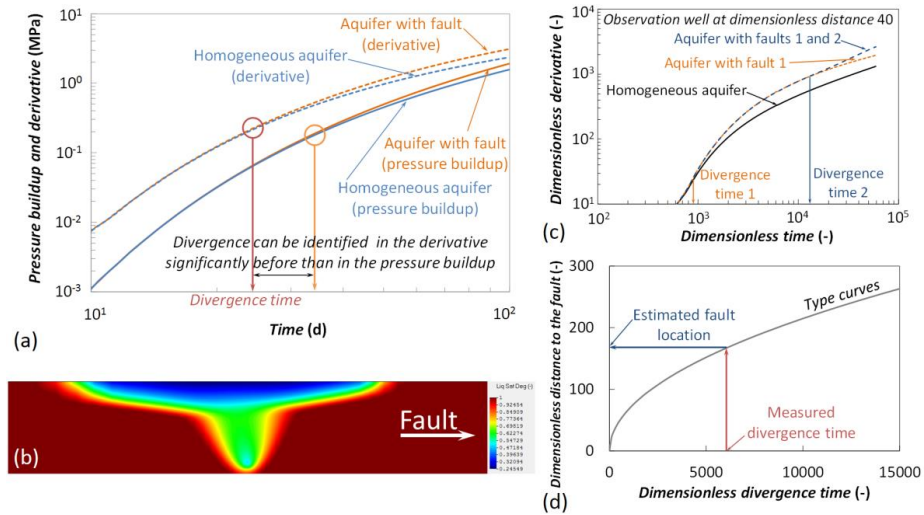
Figure 10: (a) Concept of the continuous characterization technique proposed by Vilarrasa et al. (2017c) to detect and locate low-permeable faults using diagnostic plots; (b) asymmetric CO_2 plume as a result of the additional pressurization caused by a low-permeability fault, which displaces CO_2 towards the opposite direction of the fault; (c) detection of multiple faults by updating the conceptual model of the site and comparing field measurements with predictive simulations; and (d) estimation of the fault location from the measured divergence time in the derivative of the pressure evolution using type curves.